

# Dress Anyone: A Method & Dataset for 3D Garment Retargeting

Anonymous 3DV submission

Paper ID 386

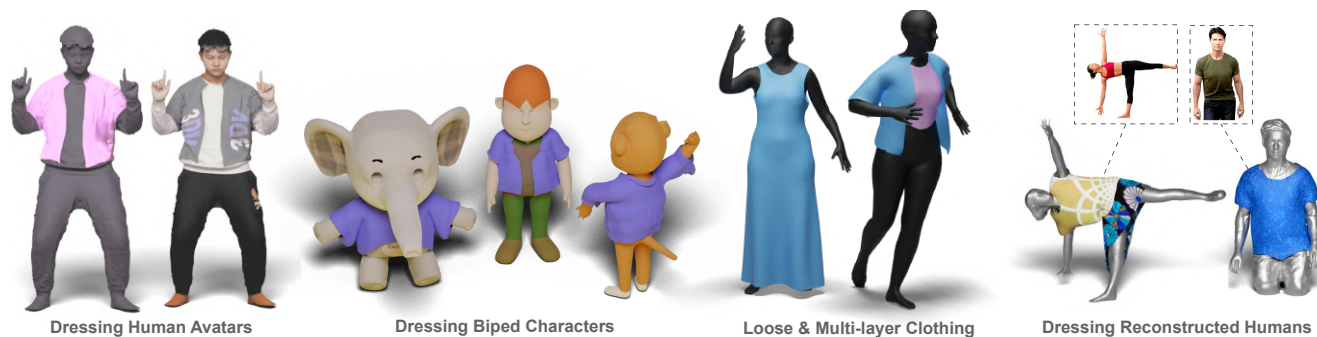


Figure 1. Our framework can retarget 3D (loose/multi-layer) garments on non-parametric meshes in arbitrary pose & shape.

## Abstract

001 *3D garment retargeting for digital characters & avatars*  
 002 *involves non-rigid deformation of a 3D garment mesh to*  
 003 *plausibly fit the target body mesh in a different pose. Exist-*  
 004 *ing neural methods for garment simulation/draping make*  
 005 *assumption that the 3D garment is initially fitted over the*  
 006 *3D body, and generally require a canonicalized represen-*  
 007 *tation of garments, limiting them to parametric settings.*  
 008 *In this paper, we present a novel approach to achieve 3D*  
 009 *garment retargeting under non-parametric settings. We*  
 010 *propose a novel isomap-based representation to first esti-*  
 011 *mate robust correspondences between garment and body*  
 012 *mesh to achieve an initial coarse retargeting, followed by a*  
 013 *fast and efficient neural optimization, governed by Physics-*  
 014 *based constraints. The proposed framework enables a fast*  
 015 *inference pipeline and quick optimization for any 3D gar-*  
 016 *ment. We perform extensive experiments on publicly avail-*  
 017 *able datasets & our new dataset of 3D clothing and report*  
 018 *superior quantitative and qualitative results in comparison*  
 019 *to SOTA methods, while demonstrating new capabilities.*

## 020 1. Introduction

021 3D garment modeling for digital characters & avatars  
 022 finds several applications in fashion, e-commerce, gaming,  
 023 movies, and AR/VR. One such useful application is 3D  
 024 Virtual Tryon, i.e. retargeting 3D digital garments on

various 3D characters/avatars. Given a 3D polygonal mesh 025  
 representation of a garment and a *biped* target body, the 026  
 objective is to repose and deform the garment mesh to *fit* 027  
 the target body mesh in a new pose while inducing pose 028  
 dependent high frequency geometrical details on garment 029  
 surface, in a plausible manner. This task is challenging 030  
 due to the articulated nature of the target body, topological 031  
 variations in garments across different categories, and 032  
 the complex non-rigid deformations caused by physical 033  
 interactions between the garment and body (e.g., collisions) 034  
 as well as external factors (e.g. gravity). 035

Traditionally, Physics-Based Simulations (PBS) is used 036  
 to simulate 3D garments on a body undergoing non-rigid 037  
 deformations [1, 20, 32, 33]. However, PBS assumes 038  
 that the initial garment mesh is already *fitted* (in the same 039  
 pose) to the underlying body before modeling the physical 040  
 interactions between them. Additionally, PBS-based 041  
 approaches often suffer from numerical instability, incur 042  
 high computational costs, are difficult to parallelize, and 043  
 require manual tuning of simulation parameters [5]. 044

Advancement in human modelling and garment digitization 045  
 has led to the emergence of several learning-based solutions 046  
 for 3D garment simulation [3, 5, 13, 14, 21, 39, 44]. In 047  
 particular, the introduction of Parametric body models, 048  
 such as SMPL [29], offers a convenient way to deal with 049  
 the articulation of the human body as well as garments, 050  
 051  
 052

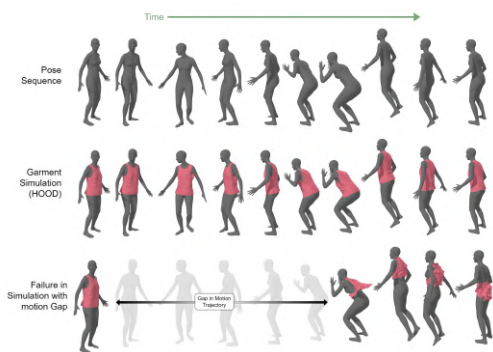


Figure 2. Neural simulation methods like HOOD[13] fail to directly retarget garments when there is gap in motion trajectory.

up to an extent. Recent developments in this direction have led to a plethora of self-supervised neural garment simulation approaches [6, 13, 14, 45]. These methods focus on modeling realistic garment deformation as the underlying body gradually changes the pose over an animated sequence. While these methods provide plausible modeling of pose-specific deformation and wrinkles by learning physics-based constraints, they require a continuous trajectory of the underlying body going from an initial pose to a final pose for training. The primary reason is that pose information from previous states of the underlying body along its trajectory is required to calculate simulation-specific parameters, such as velocity and acceleration, for the current pose. Consequently, when attempting to directly retarget the 3D garment from one arbitrary pose to another, these methods fail drastically due to the absence of motion or trajectory information between the initial garment pose and the target body pose. Figure 2 shows one such failure case of HOOD [13] in case of garment retargeting.

On the other hand, methods such as DIG [22] and DrapeNet [10] address aforementioned limitation by learning skinning weights to deform the *unposed* garment to an arbitrary pose in a self-supervised manner. However, to perform retargeting, the garment should be *unposed* (in a canonical T-pose), represented as a latent code of a large embedding space of garments (learned using supervision [10]). Recently proposed ISP [23] follows a similar approach to drape multi-layer garments, however, it assumes sewing-pattern representation of digitally created synthetic garments. Additionally, all of the aforementioned methods cannot support draping/retargeting the garment onto non-parametric human avatars or more general biped characters. Moreover, the intrinsic details of the garments (e.g. pocket, pleats, buttons etc.) are not directly preserved and are lost in the simulation.

In this work, we propose an optimization-based approach, bridging the aforementioned gaps for retargeting 3D parametric/non-parametric garments from any arbitrary pose over a target body model (parametric, non-parametric human avatar, biped characters) in a different pose, as shown in Figure 1. Given a 3D garment and a target human body as polygonal meshes, we first estimate the coarse correspondences between the two for the initial *fit*. Since existing correspondence matching methods [11, 12, 25, 28, 43] don't handle different non-rigidly deformed topologies (garment and body), we propose a novel *Isomap*-based representation, which builds upon SMPL to provide an initial non-rigid placement of the garment around the target body as a coarse retargeting initialization. We then perform a Laplacian-based detail transfer step [42] to preserve the high-fidelity geometric details (pleats, pockets, etc.) of the input garment and integrate it with the retargeted coarse garment. Finally, we employ a tiny-MLP to obtain refined pose-dependent garment deformations by efficiently optimizing for Physics-based constraints for the target pose, in a matter of seconds. Though there are several learning-based methods for generalized draping/simulation [6, 10, 22, 35, 39], all of them only work on a parametric body and need to be trained on a large collection of non-parametric target body meshes to support arbitrary out-of-distribution human avatars/scans. Our optimization-based approach provides a fast inference & quick optimization for any garments, while overcoming the aforementioned limitations. Moreover, once the tiny-MLP is optimized, it can be integrated into other differentiable pipelines (e.g. multi-view garment geometry optimization via differentiable rendering [27]). Unlike existing methods [7, 10, 22], our framework doesn't require skinning weights and, therefore, retargets any arbitrary non-parametric 3D garment on any parametric or non-parametric target body. Our key contributions are:

- We propose a novel framework for retargeting 3D garments in arbitrary pose onto parametric/non-parametric avatar, while handling loose and multilayer clothing.
- We propose a novel *Isomap*-based representation for estimating correspondences between 3D garment mesh and the target avatar mesh.
- We curate a new dataset "Real-3DVTON", comprising multiple 3D garments worn by different subjects in arbitrary poses, captured using a multi-view RGBD cameras. We plan a public release of the dataset & code.

## 2. Related Works & Background

### 3D Garment Simulation

Classical PBS based garment simulations [1, 20, 32, 33] yield good retargeting. However, they need a good initial mesh alignment and are typically computationally expensive and prone to numerical instability. Existing

142 deep learning-based methods [4, 15, 35, 40] have made  
 143 progress in this direction via supervised learning of  
 144 skinning weights of the parametric garment for draping  
 145 it onto a parametric human body. The accuracy of these  
 146 methods is driven by the amount of ground truth data  
 147 available for training. For mitigating this requirement,  
 148 methods such as [5, 6, 37, 39, 50] adopted physics-inspired  
 149 constraints for optimization, to learn a *per garment* model  
 150 in a self-supervised fashion. However, skinning-based  
 151 deformations fail to handle loose clothing, since they  
 152 initialize skinning weights from underlying SMPL. A very  
 153 recent work [7] addresses this limitation by employing an  
 154 RBF-kernel over skinning weight-initialization, based on  
 155 the distance of the garment from the underlying parametric  
 156 body, however, it requires training for a fixed garment over  
 157 a large dataset of parametric body animation sequences  
 158 [31]. Other methods [13, 19, 21, 24, 45] aim towards a  
 159 better generalization across different garment categories.  
 160 HOOD [13] proposed a hierarchical graph-based approach  
 161 extending [36] to learn skinning-free garment simulation  
 162 over across different garment categories. One major  
 163 criticism of the aforementioned method is the requirement  
 164 of a perfect initial fitting of the 3D garment over the  
 165 underlying body. Consequently, they are not suitable for  
 166 retargeting garments from one arbitrary pose directly to  
 167 another pose without going through intermediate body  
 168 poses. Another major limitation of PBS inspired neural  
 169 methods is that they only handle parametric body meshes  
 170 and unlike classical PBS-based methods, do not support  
 171 simulation over non-parametric meshes.

### 172 173 3D Garment Draping/Retargeting

174 The problem of 3D Garment Draping/Retargeting is dif-  
 175 ferent from simulation in the sense that it aims to retarget  
 176 a given 3D garment in an initial static pose directly to a  
 177 different final static body pose. Unlike simulation, this  
 178 problem doesn't depend on the availability of intermediate  
 179 dynamic pose trajectory between the initial and final pose.  
 180 One naive approach to tackle this problem in parametric  
 181 setting is to perform skinning of the garment using SMPL-  
 182 based skinning weights [8], however, it is only applicable  
 183 to extremely tight-fit clothing. Several methods have been  
 184 proposed [10, 22] to address this problem by learning  
 185 residual deformations over SMPL-based skinning. In  
 186 particular, given a dataset of 3D garments simulated over a  
 187 canonical SMPL body, DIG [22] follows an auto-decoding  
 188 approach for learning the skinning weights, optimized us-  
 189 ing implicit-surface learning. Though the learned skinning  
 190 weights can directly deform the garment to an arbitrary  
 191 target pose, the deformations are purely statistical in nature  
 192 and are not physically plausible. Drapenet [10] addresses  
 193 this limitation by imposing physics-based losses while  
 194 learning residual deformations over the initial SMPL-based

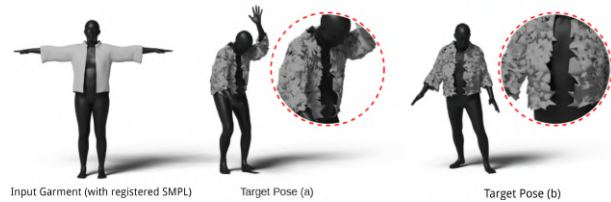


Figure 3. Coarse retargeting via nearest SMPL vertex yields noise.

195 skinning. For generalizing across different garment types,  
 196 Drapenet [10] employs a supervised training scheme to  
 197 learn a garment embedding space and then conditioning the  
 198 deformation network with the garment latent vectors. How-  
 199 ever, in order to directly pose the garment to a target both  
 200 the aforementioned methods require a 3D garment *unposed*  
 201 (*in canonical T-pose*) garment perfectly fitted over a SMPL  
 202 mesh. Moreover, their data-driven and parametric nature  
 203 restricts them from handling arbitrary non-parametric 3D  
 204 garments and target bodies. To the best of our knowledge,  
 205 there is no support for 3D draping/retargeting of non-  
 206 parametric 3D garments over non-parametric target human  
 207 avatars/characters, from one arbitrary pose to another.  
 208 Other novel view synthesis based approaches[46, 47]  
 209 require multiview input data, typically captured using a  
 210 sophisticated light-stage setup. In summary, there is a  
 211 significant gap in literature for draping any arbitrary 3D  
 212 garment from one person to another to enable 3D VTON  
 213 use case.

### 214 215 Non-rigid Correspondence Estimation

216 3D garment retargeting from one pose to another can be  
 217 seen as the problem of non-rigid shape deformation. More  
 218 specifically, given a 3D garment and a target body, the ob-  
 219 jective is to deform the 3D garment in a plausible, non-rigid  
 220 manner to fit a target body shape. In literature, methods  
 221 have been proposed [25, 43] which attempt to solve this  
 222 problem by first establishing a set of correspondences  
 223 between topologically same source and target shapes,  
 224 then using these correspondences to smoothly deform the  
 225 source shape. However, in the context of 3D garment  
 226 retargeting, the topology of the source shape (garment)  
 227 differs significantly from the target shape (body). Another  
 228 alternative is to use partial shape matching [11, 12, 28]  
 229 to find correspondences across shapes of different topolo-  
 230 gies, but such methods are typically limited to partial  
 231 regions of the same shape. We propose to address the  
 232 non-rigid deformation between two topologically different  
 233 shapes—specifically, the garment and the target body, by  
 234 leveraging SMPL-based representation to establish the  
 235 initial correspondences.

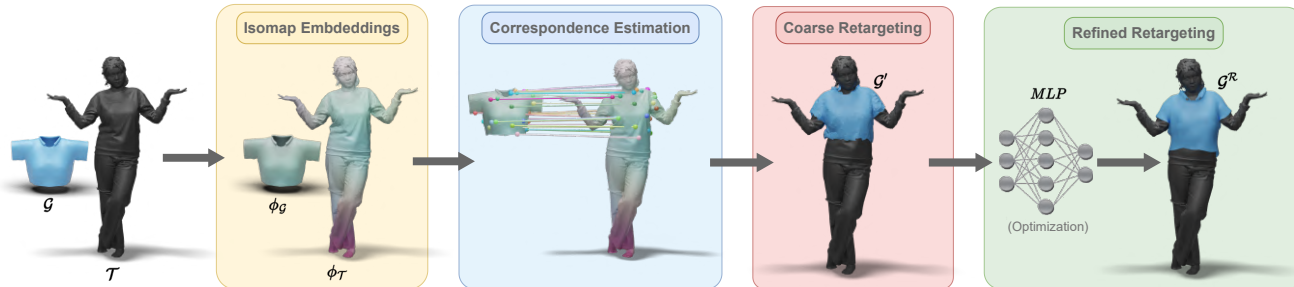


Figure 4. Outline of our proposed framework for 3D garment retargeting.

### 237 3. Methodology

238 **Figure 4** illustrates the pipeline of the proposed approach.  
 239 Given a garment mesh and a target body, we first estimate  
 240 correspondences between the two using proposed isomap  
 241 embeddings. These correspondences provide a crude idea  
 242 of how the garment should be placed around the target.  
 243 We then perform a coarse non-rigid deformation guided by  
 244 these correspondences. We also perform a Laplacian-based  
 245 detail preservation step to transfer the original details from  
 246 the input garment to the deformed garment. Finally, we re-  
 247 fine this coarse retargeting by optimizing the Physics-based  
 248 simulation losses using a tiny MLP.

#### 249 3.1. Correspondence-Guided Coarse Retargeting

250 This module aims to perform a coarse retargeting of the gar-  
 251 ment mesh over the target body by first establishing dense  
 252 surface-level correspondences between the two. Utilizing  
 253 these correspondences, we transform the garment mesh ver-  
 254 tices to align with the target body mesh vertices. The key  
 255 idea is to establish dense correspondences that can provide a  
 256 *coarse* understanding of how the garment should be draped  
 257 on the target body; e.g., sleeves going around the arms,  
 258 the collar going around the neck etc. SMPL [29], being  
 259 a parametric body model, is a natural choice for acting as  
 260 a medium for establishing dense surface correspondences,  
 261 as it can easily model variations in human shapes & poses.  
 262 Therefore, we first perform dense non-rigid registration of  
 263 both garment and target body mesh with the SMPL mesh,  
 264 as shown in **Figure 5**. It is important to note that, un-  
 265 like other methods [10, 22] which require initial garment  
 266 mesh with perfectly registered SMPL mesh, our approach  
 267 can deal with noise in SMPL registration as we use it only  
 268 to achieve initial coarse retargeting of garments (see **Fig-**  
 269 **ure 5(c)**).

270 Let the garment mesh be  $\mathcal{G}$ , target body mesh be  $\mathcal{T}$  and  
 271 their corresponding SMPL meshes be  $\mathcal{M}_{\mathcal{G}}$  &  $\mathcal{M}_{\mathcal{T}}$ , respec-  
 272 tively. Establishing correspondences between  $\mathcal{G}$  and  $\mathcal{T}$  sim-  
 273 ply means for each vertex  $v_i \in \mathbb{R}^3$  of  $\mathcal{G}$ , locating a 3D point  
 274  $x_i \in \mathbb{R}^3$  on the surface of  $\mathcal{T}$ , where  $v_i$  should be placed.  
 275 One can perform simple skinning of the garment by in-

276 terpolation the skinning weights of the underlying SMPL  
 277 mesh. However, that only allows re-posing the garment into  
 278 various poses, not in retargeting to different subjects, and  
 279 would also fail for loose garments. Alternatively, a naive  
 280 way would be to find out the nearest SMPL vertex for the  
 281 point on the garment and associate it with the corresponding  
 282 nearest SMPL vertex to the human scan, but this approach  
 283 produces a lot of local noise as an SMPL vertex can be as-  
 284 sociated to multiple garment/scan vertices (see **Figure 3**).

285 To mitigate the aforementioned issues and produce a lo-  
 286 cally smooth retargeting, we first define global features  $\phi_i$   
 287 for each vertex  $q_i$  of the SMPL meshes  $\mathcal{M}_{\mathcal{G}}$  &  $\mathcal{M}_{\mathcal{T}}$ . For  
 288 a given SMPL mesh  $\mathcal{M}$  with  $\mathcal{V}_s$  number of vertices, the  
 289 task is to estimate a feature vector  $\phi_{smpl} = [\phi_1, \phi_2, \dots, \phi_{\mathcal{V}_s}]$   
 290  $\phi_{smpl} \in \mathbb{R}^{\mathcal{V}_s \times d}$ , where  $\phi_i \in \mathbb{R}^d$ .  $\phi_{smpl}$  is the same  
 291 for any SMPL mesh registered with any garment or body,  
 292 i.e.  $\phi_{smpl} = \phi_{\mathcal{M}_{\mathcal{G}}} = \phi_{\mathcal{M}_{\mathcal{T}}}$ . The choice of appropriate  
 293  $\phi_{smpl}$  must have the following essential properties. First,  
 294 the feature embedding  $\phi_{smpl}$  should incorporate both the  
 295 local neighborhood information while maintaining global  
 296 structural context. It should be agnostic to the position of  
 297 SMPL vertices in 3D space, which means these features do  
 298 not vary based on the pose or shape of SMPL. Moreover,  
 299  $\phi_{smpl}$  should be continuous over the surface of SMPL mesh  
 300 to ensure locally smooth encoding of neighborhood infor-  
 301 mation. Finally, it should be concise yet representation-rich  
 302 to uniquely characterize the associated surface, especially  
 303 when extrapolating to the registered garment mesh or target  
 304 body mesh. We experimented with existing representations  
 305 such as CSE [34] and BodyMap [16] to serve the need for  
 306  $\phi_{smpl}$ , as they promise to encode global structural infor-  
 307 mation. However, we empirically found them to produce false  
 308 matching due to the repetition of extrapolated features due  
 309 to very low dimensionality (we provide a detailed study re-  
 310 garding this in the supplementary).

#### 311 Isomap Embeddings

312 Keeping aforementioned issue in mind, we develop a new  
 313 strategy to establish correspondence across different gar-  
 314 ments and human body via SMPL, leveraging the intrinsic  
 315 geometry-based Isomap Embeddings [18]. We first encode  
 316

317 local neighborhood information by computing the pairwise  
318 geodesic distance matrix,  $|\mathbb{D}_{geo}| = \mathcal{V}_s \times \mathcal{V}_s$ , for all pairs of  
319 vertices  $(q_i, q_j)$  of the SMPL mesh; i.e.

$$320 \quad \mathbb{D}_{geo}^{ij} = geodist(q_i, q_j) \quad (1)$$

321 To incorporate global information, we use isometric  
322 mapping to fit the vertices of SMPL mesh onto a  $d$   
323 dimensional manifold by extending metric multi-dimensional  
324 scaling (MDS) based on  $\mathbb{D}_{geo}$ . This gives us a  $d$ -  
325 dimensional representation of each SMPL vertex  $q_i$ , i.e.  
326  $\phi_{smpl}$  Figure 5(a). We empirically found that setting  $d=128$   
327 ensures sufficient dimensionality to avoid repetitions while  
328 extrapolating on the target or registered mesh.

329 Once we have a global feature embedding  $\phi_{smpl}$ , the fea-  
330 ture embedding  $\phi_{\mathcal{G}}$  for each vertex  $v_i$  of the garment mesh  
331  $\mathcal{G}$  is computed as follows:

$$332 \quad \phi_{\mathcal{G}}^i = \frac{\sum_{j=1}^k [\phi_{\mathcal{M}_{\mathcal{G}}}^j / \|v_i - q_j\|^2]}{\sum_{j=1}^k [1 / \|v_i - q_j\|^2]}; q_j \in \mathcal{N}^i \quad (2)$$

$$333 \quad \mathcal{N}^i = [q_1, q_2, \dots, q_k] \quad (3)$$

335 where,  $\|\cdot\|^2$  is the  $\mathbb{L}_2$  distance,  $q_j$  is a vertex of the un-  
336 derlying SMPL mesh  $\mathcal{M}_{\mathcal{G}}$  &  $j^{th}$  nearest neighbor of  $v_i$  in  
337 Euclidean space; and  $|\mathcal{N}^i| = k = 32$  (set empirically).  
338 Similarly, we compute  $\phi_{\mathcal{T}}$  by extrapolating  $\phi_{\mathcal{M}_{\mathcal{T}}}$  based on  
339  $k$ -nearest neighbor distance. We term these extrapolated  
340 features  $\phi_{\mathcal{G}}$  and  $\phi_{\mathcal{T}}$  as **Isomap Embeddings**. These *Isomap*  
341 *Embedding* are common across garments and target bodies  
342 as shown in Figure 5(e) & (f).

343 For an arbitrary point on the garment, an initial target  
344 3D point on the target is located via the estimated *Isomap*  
345 *Embedding vectors*. We first perform an initial retargeting  
346 to *coarsely* position the garment around the target body. In  
347 particular, for each vertex  $v_i$  of  $\mathcal{G}$ , the corresponding 3D tar-  
348 get location  $x_i$  in the vicinity of  $\mathcal{T}$  is estimated as follows:

$$349 \quad x_i = \frac{\sum_{j=1}^k [u_j / \|\phi_{\mathcal{G}}^i - \phi_{\mathcal{T}}^j\|^2]}{\sum_{j=1}^k [1 / \|\phi_{\mathcal{G}}^i - \phi_{\mathcal{T}}^j\|^2]}; \phi_{\mathcal{T}}^j \in \mathcal{N}^i \quad (4)$$

$$350 \quad \mathcal{N}^i = [\phi_{\mathcal{T}}^1, \phi_{\mathcal{T}}^2, \dots, \phi_{\mathcal{T}}^k]; \phi_{\mathcal{T}}^j \in \mathcal{N}^i \quad (5)$$

352 where,  $u_j$  is the vertex of target mesh  $\mathcal{T}$  corresponding  
353 to  $\phi_{\mathcal{T}}^j$ ,  $\mathcal{N}^i$  the set of  $k$ -nearest neighbors of  $\phi_{\mathcal{G}}^i$  in  $\phi_{\mathcal{T}}$ , and  
354  $|\mathcal{N}^i| = k = 32$ . We replace the vertices  $v_i$  of  $\mathcal{G}$  with corre-  
355 sponding  $x_i$ , coarsely retargeting the garment mesh around  
356 the target mesh  $\mathcal{T}$ .

### 358 **Garment Detail Preservation**

359 The coarse retargeted garments lack the original details like  
360 wrinkles, pleats, and collars. We take inspiration from [42],  
361 which relies on the Laplacian Matrix to encode the high-  
362 fidelity geometric details of the mesh. For given input gar-  
363 ment mesh  $\mathcal{G}$  with  $V_{\mathcal{G}} = \{v_1, v_2, \dots, v_N\} \in \mathbb{R}^3$  where  $\mathcal{N}$  is

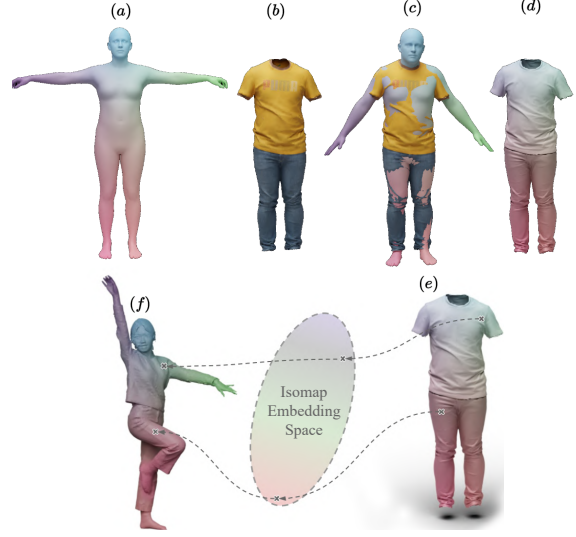


Figure 5. Isomap embedding estimation for arbitrary 3D scans: (a) SMPL mesh with per-vertex Isomap embeddings; (b) Input 3D garment(s); (c) SMPL registered with the input garment(s); (d) Isomap embeddings transferred to the input garment.

the total number of vertices, let  $\mathcal{G}'$  be the coarsely retargeted  
364 garment mesh. For each vertex  $v_i$  let,  $\mathcal{N}_i = \{j | (i, j) \in K\}$   
365 be the neighborhood ring directly connected to  $v_i$  and de-  
366 gree  $d_i$  be the number of vertices in  $\mathcal{N}_i$ . The cotan Lapla-  
367 cian coordinate per vertex is given as:  
368

$$369 \quad \delta_i(v_i) = v_i - \frac{1}{a_i} \sum_{j \in \mathcal{N}_i} (\cot \alpha_{ij} + \cot \beta_{ij})(v_i - v_j) \quad (6)$$

where  $a_i$  is the local area element,  $\alpha$  and  $\beta$  are the opposite  
370 angles of the faces on either side of the edge  $ij$ .  
371

372 In order to integrate the high-fidelity geometric details  
373 from the input garment onto retargeted garment, we first  
374 calculate the cotan Laplacian Matrix  $L_{\mathcal{G}}$  and Laplacian co-  
375 ordinates  $\delta_{\mathcal{G}}$  of the input mesh  $\mathcal{G}$ . For the coarsely tar-  
376 getted mesh  $\mathcal{G}'$ , we sort the vertices based on their distance  
377 to the underlying SMPL mesh  $\mathcal{M}_{\mathcal{T}}$  and choose the clos-  
378 est vertices as anchor points. The Laplacian matrix is re-  
379 computed as  $\hat{L} = [L_{\mathcal{G}}^T, \mathbf{1}_i]^T$  where  $\mathbf{1}_i$  is the one hot en-  
380 coding with  $i^{th}$  column value set to one. The Laplacian  
381 coordinates are recomputed as  $\hat{\delta} = [\delta_{\mathcal{G}}, v_i]^T$  where  $v_i$  are  
382 the anchor points. By solving a linear system of equation  
383  $V^{\mathcal{G}'} = \hat{L}^{-1} \hat{\delta}$ , we obtain the updated retargeted mesh  $\mathcal{G}''$   
384 with high fidelity details. Selecting only the close-body ver-  
385 tices as anchors, the loose garment details are also preserved  
386 from the original garment mesh (subsection 5.3).

### 387 **3.2. Refined Retargeting via Optimization**

388 The coarsely retargeted garment  $\mathcal{G}''$  still lacks pose-specific  
389 deformations, e.g. the wrinkles and folds formed when a

garment drops under the effect of gravity. These deformations can be obtained by Physically simulating the coarsely retargeted garment onto the static target body. While classic physics-based cloth simulations are more accurate, they are computationally expensive, difficult to parallelize and often prone to numerical instability. Neural cloth simulation methods like [6, 13] could be an alternative to classical simulations, however, they only handle SMPL. To avoid large-scale, resource-intensive training on diverse garment categories, and more importantly, due to the lack of any large, standard dataset of diverse non-parametric target meshes, we resort to an optimization-based approach for physics-guided deformation.

The coarsely retargeted garment mesh from previous step  $\mathcal{G}''$  with vertices  $V_{\mathcal{G}''}$  needs to be simulated on the static target body  $\mathcal{T}$ . We employ a *tiny* Multi-Layer Perceptron (MLP) network proposed in [41] to predict per-vertex deformation to simulate the garment. For each vertex  $V_i^{\mathcal{G}''}$  of the refined retargeted garment  $\mathcal{G}^R$ , a  $\Delta x_i \in \mathbb{R}^3$  is predicted by the MLP. The vertex position of the final simulated garment mesh  $\mathcal{G}^R$  is given as  $v_i^{\mathcal{G}^R} = v_i^{\mathcal{G}''} + \Delta x_i$ . The predicted deformations are optimized via following constraints:

$$L_{total} = \lambda_1 L_{strain} + \lambda_2 L_{bend} + \lambda_3 L_{gravity} + \lambda_4 L_{collision} + \lambda_5 L_{pin} \quad (7)$$

where,  $L_{strain}$ ,  $L_{bend}$  &  $L_{gravity}$  are taken from [13] and we adopt Collision loss  $L_{collision}$  from [26]. Pinning loss  $L_{pin}$  from [10] is used to avoid slipping of certain garment parts, e.g. straps, trouser-waist, etc., due to gravity.

## 4. Experimental Setup

**Implementation Details:** We use open-source frameworks, e.g. Trimesh[9] and Open3D[51] for implementing correspondense-guided coarse retargeting. The refined retargeting is implemented in PyTorch. We use Siren [41] as the tiny-MLP, with 3 hidden layers and 256 neurons per layer. For each garment and target body mesh pair, we optimize the refined retargeting module for  $5k$  iterations, with a learning rate of  $1e^{-5}$  using Adam optimizer. The optimization takes around 15-20 seconds for a garment mesh with  $\sim 3.5k$  vertices on an NVIDIA RTX 4090 GPU. For Equation 7, the weights  $\{\lambda_1, \lambda_2, \lambda_3, \lambda_4, \lambda_5\}$  are empirically set to  $\{1, 0.01, 1, 500, 1000\}$ .

**Public Datasets:** For qualitative comparisons, we use the garments from popular datasets e.g. CLOTH3D[2] and VTO [38] datasets. For the parametric setting, we use SMPL meshes from AMASS [31] dataset. To quantitatively evaluate our approach, we take simulated 3D garments from CLOTH3D [2] as ground truth. For non-parametric setting, we use real human scans from THuman2.0 [49] and biped cartoon characters from 3DBiCar [30] dataset to demonstrate qualitative results.

Table 1. Benchmarking on Real-3DVTON dataset

Garment Type	CD ↓	P2S ↓	IR Ratio % ↓
Top	0.03660	0.14654	0.75695
Bottom	0.02368	0.11997	2.9165

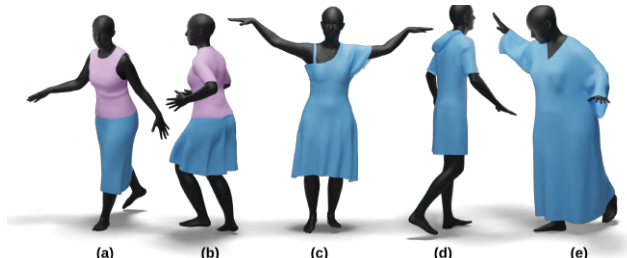


Figure 6. Our proposed framework can handle loose garments.

**Real-3DVTON (Our Dataset):** As stated in Sec. 1, there is a need for real-world dataset to evaluate 3D garment retargeting, which contains a real 3D garment draped on real 3D human in different poses. To bridge this gap we captured real garments draped onto 15 human subjects with varied body shapes, with 44 unique garments, distributed across 255 data samples in total. For every sample, a subject is scanned in 5 different poses, wearing the same garment, using a static multi-view capture setup with 7 Azure Kinect RGBD cameras. To obtain final mesh reconstructions we employ multiview Kinect Fusion[17] on the captured RGBD data, which are then post-processed in Meshlab for noise-rectification to obtain clean, UV-parametrized garment meshes. Additionally, we perform SMPL registration for each mesh to approximate the pose & shape for future use. Our dataset captures realistic noise & topological deformations of real-world garments. We believe our dataset can prove to be extremely useful in the progress of the 3D-VTON domain. We benchmark this data with our proposed method in Table 1. Please refer to supplementary for images of our dataset and additional results of our garments retargeted to avatars from THuman 2.0 [49].

**Evaluation Metrics:** To quantitatively evaluate our proposed approach, we report widely used metrics like Chamfer Distance(CD), Interpenetration Ratio(IR) and Point-to-Surface Distance(P2S). Please refer to the supplementary material for more details about these metrics.

## 5. Results & Evaluation

### 5.1. Qualitative Evaluation

**Qualitative Comparison:** Figure 7 shows qualitative comparison of our method with Drapenet[10], where our method preserves original garment details (e.g. collar) while achieving better draping quality. Similarly, Figure 8

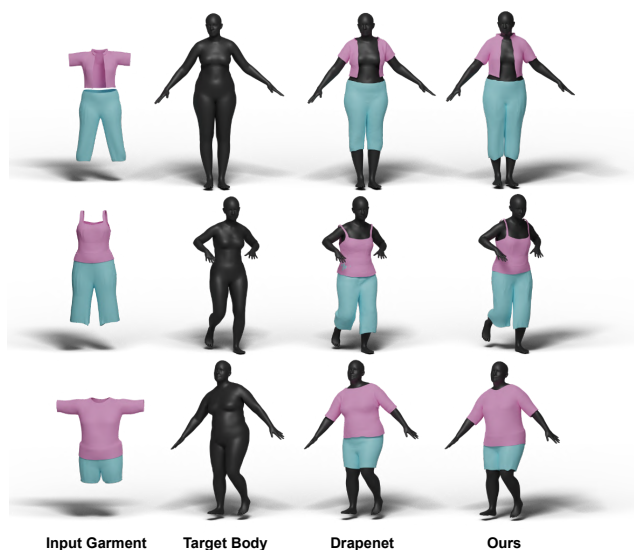


Figure 7. Qualitative comparison with DrapeNet[10]

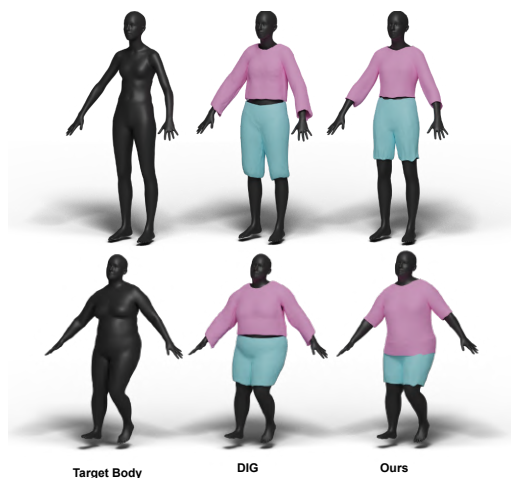


Figure 8. Qualitative comparison with DIG[22]

shows the comparison with DIG[22], where a lot of irregular deformations can be seen on the garment, while we achieve far superior retargeting. Please note that, since DIG authors do not provide inference code for arbitrary garments, we use the closest latent code to the input garment. Unlike DIG & Drapenet, we do not need to train on a large canonicalized garment dataset.

**Non-Parametric 3D Garment Retargeting:** Figure 1 highlights the capability of our method to retarget 3D garments onto any arbitrary parametric/non-parametric target mesh. Here, we also retarget 3D garment onto a 3D human mesh reconstructed from images (using [48, 52]) in a complex yoga pose. Figure 6 demonstrates that our method can effectively drape extremely loose garments from VTO [38] dataset really well. Figure 10 shows CLOTH3D garments



Figure 9. We are retargeting Cloth3D garment samples on 3DBiCar [30] dataset. Notice that our method handles varying shapes and variations in body proportions of the Biped characters.

Table 2. Quantitative Evaluation with Drapenet [10].

Module	Garment Type	CD ↓	P2S ↓	IR Ratio % ↓
DrapeNet	Top	0.2722	<b>0.0085</b>	<b>0.3752</b>
	Bottom	0.2897	0.0150	<b>1.1931</b>
Ours	Top	<b>0.00136</b>	0.01499	0.6857
	Bottom	<b>0.00054</b>	<b>0.0089</b>	1.7593

on real scans from THuman2.0 dataset. *Please, refer to the supplementary for extended results.*

**Multi-layered Clothing:** Once we have a garment draped on a target mesh, we can treat both the target and draped garment as a single mesh, and re-compute the Isomap Embeddings following the steps in Figure 5. This allows us to retarget multilayered garments as shown in Figure 11.

**Dressing Bipedes from 3DBiCar Dataset:** As shown in [30], our Isomap embeddings can be adopted for retargeting garments on biped characters. We show results of Cloth3D garments draped on samples from dataset proposed in Figure 9. *Please refer to supplementary regarding the Isomap embedding computation for 3DBiCar sample.*

## 5.2. Quantitative Evaluation

We report quantitative comparison with Drapenet[10] on CLOTH3D dataset in Table 2. We randomly sample 160 simulation sequences (80 topwear and 80 bottomwear). For each sequence, we randomly sample 5 timesteps (frames), resulting in 800 cloth-body paired meshes. Though P2S for



Figure 10. Results of Cloth3D garments draped on THuman 2.0 [49] human meshes in different poses and shapes.



Figure 11. Retargeting multi-layer garments on a single target.

Table 3. Ablative analysis of our pipeline.

Stages	Garment Type	CD x 10 <sup>-3</sup> ↓	P2S x 10 <sup>-3</sup> ↓	IR % ↓
Coarse	Top	1.071	16.74	1.046
	Bottom	0.574	12.67	2.110
Detail Transfer	Top	<b>0.902</b>	<b>13.53</b>	3.515
	Bottom	<b>0.495</b>	<b>8.950</b>	4.373
Refined	Top	1.360	14.99	<b>0.685</b>
	Bottom	0.547	8.992	<b>1.759</b>

506 both our method and drapenet is comparable, Chamfer Dis-  
 507 tance (CD) for Drapenet is significantly large due to its sus-  
 508 ceptibility towards outliers. We observe that for Drapenet,  
 509 good initial skinning of canonical garment to the target pose  
 510 is important, and any noise in skinning results in outlier ver-  
 511 tices which contribute towards larger values of CD. Inter-  
 512 penetration ratio (IR) for Drapenet is lower because it com-  
 513 putes residual deformations over initial skinning deforma-  
 514 tions (usually pointed away from the body). However, skin-  
 515 ning suffers from the aforementioned issue and also limits  
 516 applicability to loose and non-parametric garments. On the  
 517 other hand, we try to empirically balance the trade-off be-  
 518 tween collision loss and plausible deformations to support  
 519 non-parametric meshes. *Please refer to supplementary for*  
 520 *further discussion.*

### 521 5.3. Ablation Study

522 We discuss ablative analysis of all key component/stages in  
 523 our proposed pipeline. In Table 3, we report CD, P2S and IR  
 524 under the same experimental settings as quantitative evalua-  
 525 tion. While the detail preservation step yields lower CD and  
 526 P2S, it has a very high IR values compared to coarse retar-  
 527 geting as a side-effect of retaining original garment details.  
 528 The refined retargeting achieves skinning-free, physically  
 529 plausible deformations at the cost of slightly higher CD &  
 530 P2S. For Laplacian-based detail transfer, Figure 12 shows  
 531 the effect of using different % of garment vertices closest  
 532 to the body as anchors. We use the top 20% of the closest  
 533 vertices in the case of loose garments like skirts and 40%  
 534 for other relatively tighter clothing.

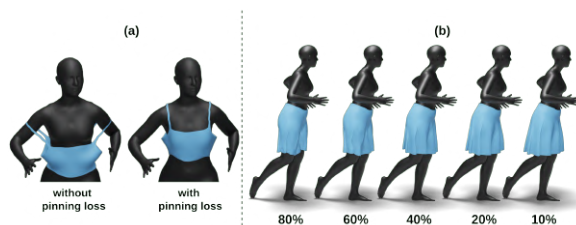


Figure 12. (a) Importance of pinning loss to avoid slipping. (b) The % of garment vertices chosen as anchors for detail transfer.

## 6. Conclusion

535 We present a novel non-parametric 3D garment retarget-  
 536 ing method that transfers any 3D garment mesh to any  
 537 target body using Isomap embeddings and SMPL for cor-  
 538 response, enabling support for non-parametric meshes.  
 539 Our tiny-MLP-based optimization yields physically plausi-  
 540 ble pose-specific deformations, while being fast and effi-  
 541 cient. Though our approach is highly robust to SMPL reg-  
 542 istration noise, we wish to completely remove any depen-  
 543 dence on parametric models in future. Secondly, we wish to  
 544 improve the collision loss to mitigate the small interpen-  
 545 etrations due to the soft-constraint nature of the loss. We  
 546 also wish to further speed up the optimization process to  
 547 allow realtime, video-driven garment retargeting. We be-  
 548 lieve the proposed method acts as a crucial step towards  
 549 non-parametric 3DVTON applications. 550



## References

- 551
- 552 [1] David Baraff and Andrew Witkin. Large steps in cloth sim- 607
- 553 ulation. In *Proceedings of the 25th Annual Conference on* 608
- 554 *Computer Graphics and Interactive Techniques*, page 43–54, 609
- 555 New York, NY, USA, 1998. Association for Computing Mach- 610
- 556 inery. 1, 2 611
- 557 [2] Hugo Bertiche, Meysam Madadi, and Sergio Escalera. 612
- 558 CLOTH3D: Clothed 3d humans. In *Proceedings of the Eu- 613*
- 559 *ropean Conference on Computer Vision (ECCV)*, 2020. 6 614
- 560 [3] Hugo Bertiche, Meysam Madadi, and Sergio Escalera. Pbn: 615
- 561 Physically based neural simulation for unsupervised garment 616
- 562 pose space deformation. *ACM Trans. Graph.*, 40(6), 2021. 1 617
- 563 [4] Hugo Bertiche, Meysam Madadi, Emilio Tylson, and Ser- 618
- 564 gio Escalera. Deepsd: Automatic deep skinning and pose 619
- 565 space deformation for 3d garment animation. In *Proceedings* 620
- 566 *of the IEEE/CVF International Conference on Computer Vi-* 621
- 567 *sion*, pages 5471–5480, 2021. 3 622
- 568 [5] Hugo Bertiche, Meysam Madadi, and Sergio Escalera. Neu- 623
- 569 ral cloth simulation. *ACM Trans. Graph.*, 41(6), 2022. 1, 624
- 570 3 625
- 571 [6] Ruochen Chen, Liming Chen, and Shaifali Parashar. Gaps: 626
- 572 Geometry-aware, physics-based, self-supervised neural gar- 627
- 573 ment draping. *2024 International Conference on 3D Vision* 628
- 574 *(3DV)*, pages 116–125, 2023. 2, 3, 6 629
- 575 [7] Ruochen Chen, Liming Chen, and Shaifali Parashar. Gaps: 630
- 576 Geometry-aware, physics-based, self-supervised neural gar- 631
- 577 ment draping, 2024. 2, 3 632
- 578 [8] Enric Corona, Albert Pumarola, Guillem Alenyà, Ger- 633
- 579 ard Pons-Moll, and Francesc Moreno-Noguer. Smplicit: 634
- 580 Topology-aware generative model for clothed people, 2021. 635
- 581 3 636
- 582 [9] Dawson-Haggerty et al. Trimesh library, 2019. 6 637
- 583 [10] Luca De Luigi, Ren Li, Benoît Guillard, Mathieu Salzmann, 638
- 584 and Pascal Fua. Drapenet: Generating garments and draping 639
- 585 them with self-supervision, 2022. 2, 3, 4, 6, 7 640
- 586 [11] Viktoria Ehm, Paul Roetzer, Marvin Eisenberger, Maolin 641
- 587 Gao, Florian Bernard, and Daniel Cremers. Geometrically 642
- 588 consistent partial shape matching, 2023. 2, 3 643
- 589 [12] Viktoria Ehm, Maolin Gao, Paul Roetzer, Marvin Eisen- 644
- 590 berger, Daniel Cremers, and Florian Bernard. Partial-to- 645
- 591 partial shape matching with geometric consistency, 2024. 2, 646
- 592 3 647
- 593 [13] Artur Grigorev, Bernhard Thomaszewski, Michael J. Black, 648
- 594 and Otmar Hilliges. In *Proceedings of the IEEE/CVF* 649
- 595 *Conference on Computer Vision and Pattern Recognition* 650
- 596 *(CVPR)*, 2023. 1, 2, 3, 6 651
- 597 [14] Artur Grigorev, Giorgio Becherini, Michael Black, Ot- 652
- 598 mar Hilliges, and Bernhard Thomaszewski. ContourCraft: 653
- 599 Learning to resolve intersections in neural multi-garment 654
- 600 simulations. In *ACM SIGGRAPH 2024 Conference Papers*, 655
- 601 pages 1–10, 2024. 1, 2 656
- 602 [15] Erhan Gundogdu, Victor Constantin, Shaifali Parashar, Am- 657
- 603 rollah Seifoddini, Minh Dang, Mathieu Salzmann, and Pas- 658
- 604 cal Fua. Garnet++: Improving fast and accurate static 3d 659
- 605 cloth draping by curvature loss. *IEEE Trans. Pattern Anal.* 660
- 606 *Mach. Intell.*, 44(1):181–195, 2022. 3 661
- [16] Anastasia Ianina, Nikolaos Sarafianos, Yuanlu Xu, Ignacio 662
- Rocco, and Tony Tung. Bodymap: Learning full-body dense 663
- correspondence map. In *CVPR*, 2022. 4
- [17] Shahram Izadi, David Kim, Otmar Hilliges, David 610
- Molyneaux, Richard Newcombe, Pushmeet Kohli, Jamie 611
- Shotton, Steve Hodges, Dustin Freeman, Andrew Davison, 612
- and Andrew Fitzgibbon. Kinectfusion: Real-time 3d recon- 613
- struction and interaction using a moving depth camera. In 614
- UIST '11 Proceedings of the 24th annual ACM symposium* 615
- on User interface software and technology*, pages 559–568. 616
- ACM, 2011. 6 617
- [18] Varun Jampani, Martin Kiefel, and Peter V. Gehler. Learn- 618
- ing sparse high dimensional filters: Image filtering, dense 619
- crfs and bilateral neural networks. In *Proceedings of the* 620
- IEEE Conference on Computer Vision and Pattern Recog-* 621
- nition (CVPR)*, 2016. 4 622
- [19] Dohae Lee, Hyun Kang, and In-Kwon Lee. Clothcombo: 623
- Modeling inter-cloth interaction for draping multi-layered 624
- clothes. *ACM Transactions on Graphics (TOG)*, 42:1 – 13, 625
2023. 3 626
- [20] Jie Li, Gilles Daviet, Rahul Narain, Florence Bertails- 627
- Descoubes, Matthew Overby, George E. Brown, and Lau- 628
- rence Boissieux. An implicit frictional contact solver for 629
- adaptive cloth simulation. *ACM Trans. Graph.*, 37(4), 2018. 630
- 1, 2 631
- [21] Peizhuo Li, Tuanfeng Y. Wang, Timur Levent Kesdogan, 632
- Duygu Ceylan, and Olga Sorkine-Hornung. Neural garment 633
- dynamics via manifold-aware transformers. *Computer* 634
- Graphics Forum (Proceedings of EUROGRAPHICS 2024)*, 635
- 43(2), 2024. 1, 3 636
- [22] Ren Li, Benoît Guillard, Edoardo Remelli, and Pascal Fua. 637
- Dig: Draping implicit garment over the human body, 2022. 638
- 2, 3, 4, 7 639
- [23] Ren Li, Benoît Guillard, and Pascal Fua. Isp: Multi-layered 640
- garment draping with implicit sewing patterns, 2023. 2 641
- [24] Tianxing Li, Rui Shi, Qing Zhu, and Takashi Kanai. 642
- Swingar: Spectrum-inspired neural dynamic deformation for 643
- free-swinging garments. *IEEE transactions on visualization* 644
- and computer graphics*, PP, 2023. 3 645
- [25] Yang Li and Tatsuya Harada. Leopard: Learning partial point 646
- cloud matching in rigid and deformable scenes, 2022. 2, 3 647
- [26] Yudi Li, Min Tang, Yun Yang, Zi Huang, Ruofeng Tong, 648
- Shuangcai Yang, Yao Li, and Dinesh Manocha. N-cloth: 649
- Predicting 3d cloth deformation with mesh-based networks, 650
2022. 6 651
- [27] Yifei Li, Hsiao-yu Chen, Egor Larionov, Nikolaos Sarafi- 652
- anos, Wojciech Matusik, and Tuur Stuyck. DiffAvatar: 653
- Simulation-ready garment optimization with differentiable 654
- simulation. In *Proceedings of the IEEE/CVF Conference on* 655
- Computer Vision and Pattern Recognition (CVPR)*, 2024. 2 656
- [28] O. Litany, E. Rodolà, A. M. Bronstein, and M. M. Bronstein. 657
- Fully spectral partial shape matching. *Computer Graphics* 658
- Forum*, 36(2):247–258, 2017. 2, 3 659
- [29] Matthew Loper, Naureen Mahmood, Javier Romero, Gerard 660
- Pons-Moll, and Michael J. Black. SMPL: A skinned multi- 661
- person linear model. *ACM Transactions on Graphics (Proc.* 662
- SIGGRAPH Asia)*, 34(6):248:1–248:16, 2015. 1, 4 663

- [30] Zhongjin Luo, Shengcai Cai, Jinguo Dong, Ruibo Ming, Liangdong Qiu, Xiaohang Zhan, and Xiaoguang Han. Rabbit: Parametric modeling of 3d biped cartoon characters with a topological-consistent dataset. In *Proceedings of the IEEE/CVF Conference on Computer Vision and Pattern Recognition (CVPR)*, 2023. 6, 7
- [31] Naureen Mahmood, Nima Ghorbani, Nikolaus F. Troje, Gerard Pons-Moll, and Michael J. Black. AMASS: Archive of motion capture as surface shapes. In *International Conference on Computer Vision*, pages 5442–5451, 2019. 3, 6
- [32] Rahul Narain, Armin Samii, and James F O’Brien. Adaptive anisotropic remeshing for cloth simulation. *ACM transactions on graphics (TOG)*, 31(6):1–10, 2012. 1, 2
- [33] Andrew Nealen, Matthias Müller, Richard Keiser, Eddy Boxerman, and Mark Carlson. Physically based deformable models in computer graphics. In *Computer graphics forum*, pages 809–836. Wiley Online Library, 2006. 1, 2
- [34] Natalia Neverova, David Novotný, Vasil Khalidov, Marc Szafraniec, Patrick Labatut, and Andrea Vedaldi. Continuous surface embeddings. *ArXiv*, abs/2011.12438, 2020. 4
- [35] Chaitanya Patel, Zhouyingcheng Liao, and Gerard Pons-Moll. TailorNet: Predicting clothing in 3D as a function of human pose, shape and garment style. In *Proceedings of the IEEE Conference on Computer Vision and Pattern Recognition (CVPR)*, 2020. 2, 3
- [36] Tobias Pfaff, Meire Fortunato, Alvaro Sanchez-Gonzalez, and Peter W. Battaglia. Learning mesh-based simulation with graph networks, 2021. 3
- [37] Igor Santesteban, Miguel A. Otaduy, and Dan Casas. Learning-based animation of clothing for virtual try-on. *Computer Graphics Forum*, 38, 2019. 3
- [38] Igor Santesteban, Miguel A. Otaduy, and Dan Casas. Learning-Based Animation of Clothing for Virtual Try-On. *Computer Graphics Forum (Proc. Eurographics)*, 2019. 6, 7
- [39] Igor Santesteban, Miguel A Otaduy, and Dan Casas. SNUG: Self-Supervised Neural Dynamic Garments. *IEEE/CVF Conference on Computer Vision and Pattern Recognition (CVPR)*, 2022. 1, 2, 3
- [40] Yidi Shao, Chen Change Loy, and Bo Dai. Towards multi-layered 3d garments animation. In *ICCV*, 2023. 3
- [41] Vincent Sitzmann, Julien N.P. Martel, Alexander W. Bergman, David B. Lindell, and Gordon Wetzstein. Implicit neural representations with periodic activation functions. In *arXiv*, 2020. 6
- [42] Olga Sorkine, Daniel Cohen-Or, Yaron Lipman, Marc Alexa, Christian Rössl, and H-P Seidel. Laplacian surface editing. In *Proceedings of the 2004 Eurographics/ACM SIGGRAPH symposium on Geometry processing*, pages 175–184, 2004. 2, 5
- [43] Ramana Sundararaman, Gautam Pai, and Maks Ovsjanikov. Implicit field supervision for robust non-rigid shape matching. In *Computer Vision – ECCV 2022: 17th European Conference, Tel Aviv, Israel, October 23–27, 2022, Proceedings, Part III*, page 344–362, Berlin, Heidelberg, 2022. Springer-Verlag. 2, 3
- [44] Lokender Tiwari and Brojeshwar Bhowmick. Garsim: Particle based neural garment simulator. In *Proceedings of the IEEE/CVF Winter Conference on Applications of Computer Vision (WACV)*, pages 4472–4481, 2023. 1
- [45] Lokender Tiwari, Brojeshwar Bhowmick, and Sanjana Sinha. Gensim: Unsupervised generic garment simulator. In *Proceedings of the IEEE/CVF Conference on Computer Vision and Pattern Recognition (CVPR) Workshops*, pages 4169–4178, 2023. 2, 3
- [46] Donglai Xiang, Fabian Prada, Timur Bagautdinov, Weipeng Xu, Yuan Dong, He Wen, Jessica Hodgins, and Chenglei Wu. Modeling clothing as a separate layer for an animatable human avatar. *ACM Transactions on Graphics*, 40(6):1–15, 2021. 3
- [47] Donglai Xiang, Timur Bagautdinov, Tuur Stuyck, Fabian Prada, Javier Romero, Weipeng Xu, Shunsuke Saito, Jingfan Guo, Breannan Smith, Takaaki Shiratori, Yaser Sheikh, Jessica Hodgins, and Chenglei Wu. Dressing avatars: Deep photorealistic appearance for physically simulated clothing. *ACM Transactions on Graphics*, 41(6):1–15, 2022. 3
- [48] Yuliang Xiu, Jinlong Yang, Xu Cao, Dimitrios Tzionas, and Michael J. Black. ECON: Explicit Clothed humans Obtained from Normals. In *Proceedings of the IEEE/CVF Conference on Computer Vision and Pattern Recognition (CVPR)*, 2023. 7
- [49] Tao Yu, Zerong Zheng, Kaiwen Guo, Pengpeng Liu, Qionghai Dai, and Yebin Liu. Function4d: Real-time human volumetric capture from very sparse consumer rgbd sensors. In *IEEE Conference on Computer Vision and Pattern Recognition (CVPR2021)*, 2021. 6, 8
- [50] Meng Zhang, Duygu Ceylan, and Niloy J. Mitra. Motion guided deep dynamic 3d garments. *ACM Trans. Graph.*, 41(6), 2022. 3
- [51] Qian-Yi Zhou, Jaesik Park, and Vladlen Koltun. Open3D: A modern library for 3D data processing. *arXiv:1801.09847*, 2018. 6
- [52] Heming Zhu, Lingteng Qiu, Yuda Qiu, and Xiaoguang Han. Registering explicit to implicit: Towards high-fidelity garment mesh reconstruction from single images, 2022. 7